JOURNAL OF MATERIALS SCIENCE 15 (1980) 96–102

Observations on the effect of calcium segregation on the fracture behaviour of polycrystalline alumina

R. S. JUPP, D. F. STEIN, D. W. SMITH
Department of Metallurgical Engineering, Michigan Technological University, Houghton, Michigan 49931, USA

The influence of calcium segregation to the grain boundaries of polycrystalline alumina on room temperature fracture behaviour has been investigated. In a commercial high-density single-phase alumina containing less than 5 ppm calcium by weight, thermal treatments were employed to achieve equilibrium segregation from 0.6 to 1.6 at % calcium without detectable changes in grain size (18 μm) or porosity distribution. Room temperature SENB test results revealed an inverse dependence of K_{IC} on calcium segregation levels in the range examined. Fractures were primarily intergranular in all specimens. Qualitatively, the relationship between K_{IC} and calcium segregation would be predicted from a consideration of the effect of such an ion on the interatomic spacing at the boundary. However, quantitative agreement with the model is poor, the measured effect being much greater than predicted. A relatively high K_{IC} value was achieved in a fine grained (2 μm) hot-pressed alumina containing very low levels of segregated impurities. This material exhibited substantial amounts of cleavage fracture. The higher fracture toughness of this alumina is discussed in terms of both increased intergranular and transgranular fracture stresses promoted by the relatively clean grain boundaries and small grain size, respectively.

1. Introduction

The segregation of impurities to grain boundaries in metals and alloys and the resulting embrittlement of such materials have been of considerable interest for several years [1–5]. More recent investigations [3–5] have utilized Auger electron spectroscopy (AES) to directly determine the nature and extent of such segregation. These studies have been quite successful in clarifying such phenomena as temper embrittlement in low alloy steels [4] and the embrittlement of copper by trace levels of bismuth [5].

In polycrystalline ceramic materials, where brittle intergranular fracture at low applied stress levels is generally expected, there has been little effort to evaluate the effect on mechanical behaviour of segregation of trace impurities to grain boundaries. Marcus and Fine [6] reported the detection of significant concentrations (up to 3 to 5 at %) of calcium on the intergranular fracture surfaces of a commercial high-density alumina, although the total calcium content of the material was only about 20 ppm by weight. It was suggested that this segregation resulted primarily from the distortion energy associated with the Ca^{2+} ion in residence on an Al^{3+} lattice site, since the Ca^{2+} ion is nearly twice as large (0.99 Å) as the Al^{3+} ion (0.5 Å). Subsequent investigations confirmed that calcium segregation occurred in other polycrystalline aluminas [7, 8] and an initial study was conducted to assess the effect of this segregation on room temperature fracture toughness [8]. The study indicated that calcium may have a deleterious effect on the fracture toughness of alumina, but an unequivocal interpretation was made difficult by the fact that the aluminas examined contained varying second-phase particle distributions and slightly different porosity levels.

0022–2461/80/010096–07$02.70/0

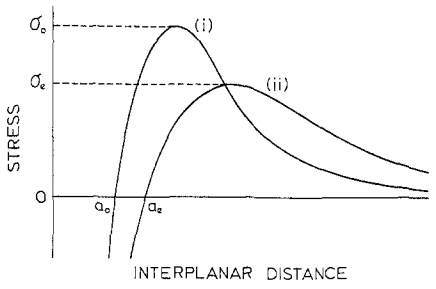

Figure 1 Schematic curves illustrating the change in cohesion between atom planes across a grain boundary effected by the segregation of impurity atoms larger than the host (curve ii). Curve i applies to a boundary without segregated impurities [9].

Qualitatively, the influence of segregation on the tendency of a material to exhibit brittle intergranular fracture behaviour can be appreciated in terms of its influence on interatomic potentials across a grain boundary, as illustrated in Fig. 1 [9]. As large atoms replace smaller host atoms at the boundary, the average interatomic spacing increases from a_0 to a_e and the potential curve shifts from (i) to (ii). If the work of fracture is relatively unchanged [9], the area under each curve is about equal and, therefore, the maximum stress (grain-boundary fracture stress) is reduced. This result can be expressed by,

$$\sigma_e = \frac{\sigma_0}{1 + \frac{1}{2} X_b \left(\frac{a_e}{a_0} - 1 \right)} \quad (1)$$

where σ_0 and σ_e are the fracture stresses associated with the clean and impure boundaries, respectively, and X_b is the atomic fraction of segregant at the boundary. Equation 1 predicts that the segregation of atoms larger than the host atom ($a_e/a_0 > 1$) will decrease the fracture stress, while atomically small segregants ($a_e/a_0 < 1$) should promote a strengthening effect.

In the absence of any physical alterations other than grain-boundary chemistry, the present study has sought to evaluate the effect of calcium segregation to the grain boundaries of polycrystalline alumina on its room temperature fracture behaviour.

2. Materials and procedure

The primary material utilized in this investigation was a commercial pressed and sintered alumina having a uniform grain size of 18 μm and a density in excess of 99% of the theoretical density of alumina (3.97 g cm^{-3}). This material had been doped with a small amount of MgO to restrict grain growth and promote sintering. Also, a vacuum hot-pressed alumina made from very high-purity zone-refined aluminium by hydrothermal methods [10] was examined in this study. This alumina was undoped and had a uniform grain size of about 2 μm and a density in excess of 99% of theoretical.

Bulk chemical analysis of the commercial alumina revealed 300 ppm Mg, 40 ppm Si and less than 5 ppm Ca by weight present as the principal impurities. The concentrations of all other impurities were less than 1 ppm. Neither calcium nor magnesium was detected in the hot-pressed alumina although a bulk silicon level of about 200 ppm was reported. The silicon was encountered as a contaminant during the hydrothermal conversion of the aluminium to Al_2O_3. All other elements were less than 1 ppm in the hot-pressed alumina.

Specimens of the commercial alumina were subjected to vacuum heat-treatments (5×10^{-6} Torr) at 1650, 1800 and 1950° C for times up to 16 h to establish equilibrium concentrations of segregants at the grain boundaries. The specimens were quenched in high-purity helium at a rate known to be substantially in excess of 600° C min^{-1}.

Scanning electron microscopy (SEM) and AES were used to study fracture surface morphology and chemistry, respectively. The AES determinations were made on surfaces produced by fracturing the aluminas in the instrument chamber under high vacuum to prevent subsequent contamination. Prior to SEM examination, the fracture surfaces were shadowed with gold–palladium to eliminate charging effects.

A relief polishing technique [11] was used to prepare specimens of the aluminas for optical microscopy determinations of grain size and second-phase particle and pore distributions. Supplementary examination of ion-milled thin sections was conducted using transmission electron microscopy (TEM).

Single edge-notched beam (SENB) specimens for room temperature fracture toughness testing were cut from the as-prepared and heat-treated aluminas using a wafering machine with a 0.048 cm thick diamond blade. These specimens were 0.25 cm × 0.25 cm × 2.5 cm and were notched to a depth of 0.056 cm. Fracture toughness testing was accomplished by four-point bend loading on an Instron testing machine at a cross-head speed of 0.005 cm min^{-1}. Plane strain fracture toughness (K_{IC}) was computed from the load–deflection

TABLE I Physical characteristics of test aluminas

Alumina	Heat-treatment	% density	Average grain size (μm)	at % Ca on grain boundaries (from	% intergranular fracture	Porosity*
Commercial	As-sintered	99 +	18	1.2	90	S, GB, 1–5 μm
Commercial	1650° C, 16 h	99 +	18	1.6	90	S, GB, 1–5 μm
Commercial	1800° C, 3 h	99 +	18	0.9	85	S, GB, 1–5 μm
Commercial	1950° C, 1 h	99 +	18	0.6	80	S, GB, 1–5 μm
Hot-pressed	As hot-pressed	99 +	2	ND (< 0.1 at %)	50	S, GB, < 1 μm

*S = nearly spherical. GB = located at grain boundaries.

curves and the sample dimensions using a standard equation for SENB specimens [12].

3. Results and discussion

3.1. Characterization of aluminas

The characteristics of the as-prepared and heat-treated aluminas with respect to microstructure, room temperature fracture mode and grain-boundary impurity levels are summarized in Table I. Heat-treatment of the commercial alumina resulted in changes in the chemical composition at the grain boundaries but no detectable alteration in grain size, density, or pore morphology. Calcium was the only impurity element detected on the fracture surfaces of the commercial alumina. No impurities were found in the regions of intergranular fracture of the hot-pressed material using scanning Auger methods.

SEM revealed that the fractures in the commercial alumina were predominantly intergranular, the incidence of cleavage increasing only slightly in the specimens heat-treated at 1800 and 1950° C. The fine-grained hot-pressed alumina exhibited substantially more cleavage fracture. Scanning electron fractographs of typical regions of these surfaces are shown in Figs. 2 and 3.

No second phase particles were discovered in either alumina by optical microscopy or TEM techniques. Because of the low impurity levels (except for silicon) in the hot-pressed material, no second phase(s) would be expected. Although many commercial aluminas contain spinel particles, the magnesium level of the commercial material used here was apparently sufficiently low to preclude the formation of such particles.

3.2. Calcium segregation

The observed change in grain-boundary calcium concentration in the commercial alumina with heat-treating temperature is the result anticipated from equilibrium segregation theory based upon saturation adsorption concepts. The McLean–Langmuir expression [13],

$$C_{gb} = \frac{C \exp\left(\frac{\Delta G}{RT}\right)}{1 + C \exp\left(\frac{\Delta G}{RT}\right)}, \qquad (2)$$

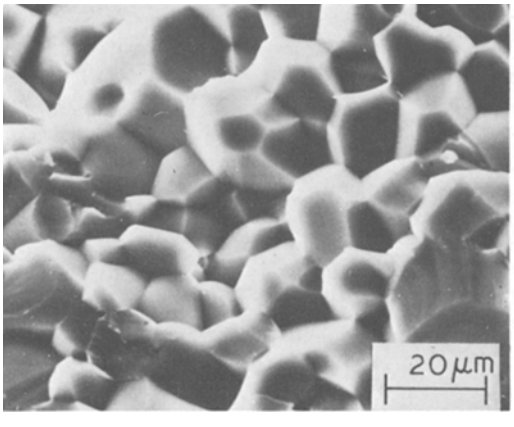

Figure 2 Scanning electron fractograph of the as-sintered commercial alumina used in this investigation (grain size = 18 μm, density > 99% theoretical). Fracture is predominantly intergranular.

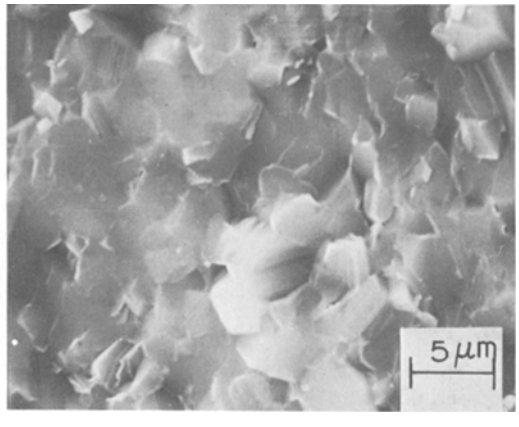

Figure 3 Scanning electron fractograph of hot-pressed alumina (grain size = 2 μm, density > 99% theoretical). Fracture represents approximately 50% cleavage (conchoidal) mode over entire specimen surface.

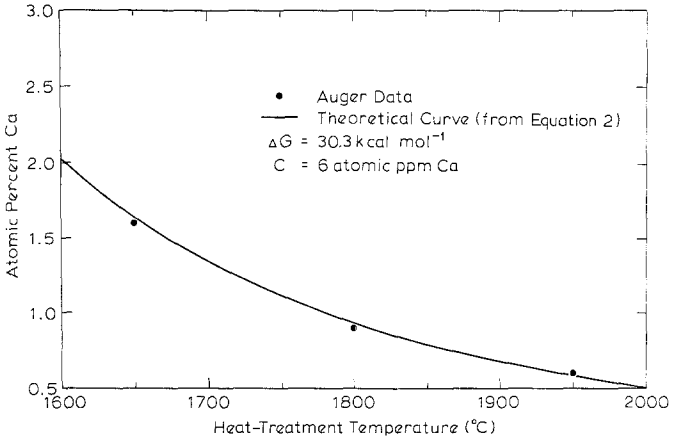

Figure 4 Concentration of calcium at the grain boundaries of commercial alumina used in this investigation as a function of heat-treating temperature (from AES measurements on fresh fracture surfaces).

predicts that the concentration of a given impurity at a grain boundary (C_{gb}) in equilibrium with a bulk (lattice) concentration of the impurity (C) will decrease with increasing temperature (T). In this expression, ΔG is the change in internal energy associated with segregation of the impurity to the grain boundary and R is the universal gas constant.

The levels of calcium segregated to the grain boundaries of the heat-treated commercial alumina specimens are listed in Table I and plotted in Fig. 4. The measured calcium levels provide an excellent fit to Equation 2 for $C = 6$ atomic ppm Ca and $\Delta G \cong 30\,\text{kcal mol}^{-1}$. A previous study concluded that ΔG for calcium segregation in alumina is about $28\,\text{kcal mol}^{-1}$ [7]. Although Equation 2 inherently assumes an infinite grain size and no interaction among the segregating impurity ions, it does provide an adequate description of calcium segregation in this very dilute and relatively coarse-grained alumina. The charge difference between the segregating Ca^{2+} ions and the Al^{3+} lattice cations is presumed to be a negligible factor in the segregation process. Recent work [14] has shown that distortion energy (proportional to the square of strain due to ion size misfit in the lattice) is the primary driving force for segregation of several impurity species in alumina, at least in those cases where the charge difference is no greater than one.

The as-sintered commercial alumina contained 1.2 at% calcium at the grain boundaries, a value which is considerably greater than would be predicted from the high sintering temperature involved (about 1950° C). Undoubtedly, additional segregation was experienced during relatively slow cooling from the sintering temperature.

No calcium was detected in the intergranular regions of the fracture surface of the hot-pressed alumina. The lower limit of detection for AES is about 0.1 at%. This would suggest that, if an equilibrium segregation level was achieved during hot-pressing, the bulk calcium concentration, based on Equation 2, was less than 0.2 atomic ppm. However, it is unlikely that the equilibrium grain-boundary calcium concentration was reached under the time–temperature conditions of hot-pressing (2 h at 1450° C). Furthermore, the fine grain size of this alumina should lead to a reduced calcium segregation level due to the substantially increased boundary area available [15]. It has also been suggested [14] that the presence of silicon in alumina reduces the level of segregated calcium for silicon contents similar to those present in this hot-pressed material. Thus, the bulk calcium concentration of this alumina was undoubtedly very low, but could have exceeded the 0.2 atomic ppm level estimated as a maximum based on equilibrium segregation theory.

3.3. Fracture behaviour

The results of the room temperature SENB fracture toughness tests on the commercial and hot-pressed aluminas are listed in Table II and plotted versus grain-boundary calcium concentrations in Fig. 5. For comparison, one data point (0.5 at% Ca) is included in Fig. 5 from a previous investigation [8]. This point represents a measured K_{IC} value from SENB tests on an MgO-doped high-density (>99%) pressed and sintered alumina containing less than 2 vol.% spinel ($MgAl_2O_4$) particles and having a uniform grain size of 9 μm. The error bars in Fig. 5 represent the extreme values obtained in each set of four measurements, as given in Table II.

An obvious trend toward improved fracture toughness with decreasing grain-boundary calcium concentration is indicated in Fig. 5. Considering

TABLE II Room temperature K_{IC} values for test aluminas (SENB specimens)

Alumina	Heat-treatment	at% Ca at grain boundary	Range of K_{IC} values (MN m$^{-3/2}$) (four tests)	Average K_{IC} (MN m$^{-3/2}$)
Commercial	1650° C 16 h	1.6	4.48–4.69	4.60
Commercial	As-sintered	1.2	4.66–4.86	4.75
Commercial	1800° C 3 h	0.9	4.78–4.97	4.87
Commercial	1950° C 1 h	0.6	4.96–5.16	5.08
Hot-pressed	As hot-pressed	ND (< 0.1 at%)	5.66–5.84	5.73

specifically the data for the commercial alumina, since no second-phase particles were present in these structures and neither the grain size nor the distribution of porosity were altered detectably by the thermal treatments employed, these data permit a self-consistent appraisal of the magnitude of the effect of this range of calcium segregation (0.6 to 1.6 at%) uniquely on the fracture toughness. Also, the data can be used to crudely test the Seah model [9] for the quantitative dependence of grain-boundary fracture stress on segregation level. This polycrystalline alumina is a suitable material for a test of this model inasmuch as the fracture mode is predominantly intergranular and no dislocation activity is encountered in the fracture of alumina at temperatures below about 800° C [16, 17].

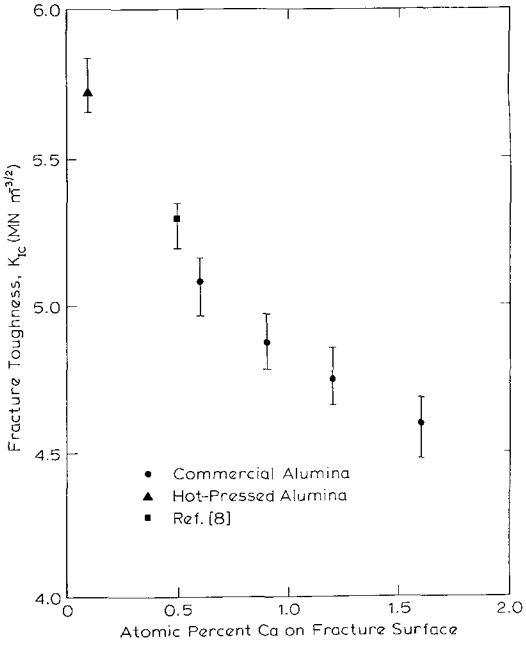

Figure 5 Dependence of room temperature fracture toughness (SENB tests) on grain-boundary calcium concentration for commercial and hot-pressed aluminas.

Equation 1 can be written,

$$\sigma_e \left[1 + \tfrac{1}{2} X_b \left(\frac{a_e - a_0}{a_0}\right)\right] = \sigma_0 .$$

Redefining a_e and a_0 as the radii of the impurity ions and host ions, respectively [9], where, for this system, $a_e(Ca^{2+}) = 0.99$ Å and $a_0(Al^{3+}) = 0.5$ Å,

$$\sigma_e [1 + 0.49\, X_b^{Ca}] = \sigma_0 . \quad (3)$$

For a comparison of the effect of any two values of X_b^{Ca},

$$\frac{\sigma_{e_1}}{\sigma_{e_2}} = \left[\frac{1 + 0.49\, X_{b_1}^{Ca}}{1 + 0.49\, X_{b_2}^{Ca}}\right]^{-1} . \quad (4)$$

For the SENB test technique and constant specimen geometry, K_{IC} will be directly related to σ. Thus,

$$\frac{K_{IC_1}}{K_{IC_2}} \approx \left[\frac{1 + 0.49\, X_{b_1}^{Ca}}{1 + 0.49\, X_{b_2}^{Ca}}\right]^{-1} . \quad (5)$$

This relationship predicts a virtually negligible variation in σ_e or K_{IC} over the range of grain-boundary calcium concentrations achieved in the commercial alumina. The predicted and measured trends in K_{IC} are given in Table III and this information is shown graphically in Fig. 6. The K_{IC} ratios are based on the value obtained for $X_b^{Ca} = 0.006$. Therefore, the apparent match between the

TABLE III Predicted and observed K_{IC} variation with X_b^{Ca}

X_b^{Ca}	$\frac{K_{IC}(X_b^{Ca} = 0.006)}{K_{IC}(X_b^{Ca})}$	
	Predicted from Equation 5	Observed
0.006	1.0	1.0
0.009	1.0015	1.0431
0.012	1.0029	1.0695
0.016	1.0049	1.1043
0.025	1.0093	–

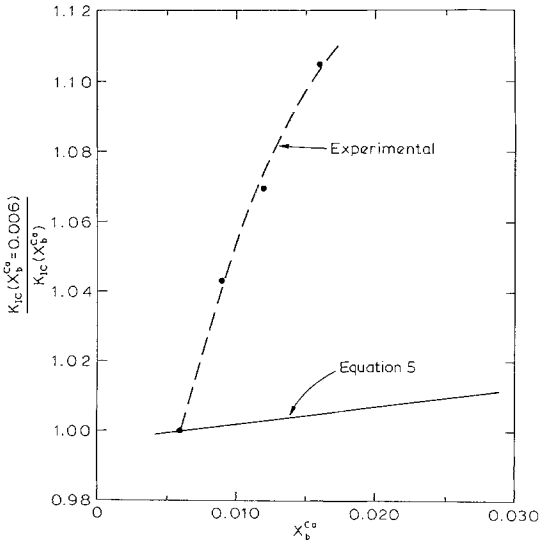

Figure 6 Experimental determination of K_{IC} variation with X_b^{Ca} compared to theory (Equation 5). Match at $X_b^{Ca} = 0.006$ is forced.

model prediction and experiment at this point is forced.

It is readily apparent that dependence of K_{IC} for intergranular fracture on the grain-boundary concentration of calcium in this alumina is much greater than estimated from Equation 5. Although the model correctly predicts the inverse nature of the dependence of grain-boundary integrity on the concentration of a large ion at the boundary, the magnitude of this effect is seriously underestimated. As noted previously, the Seah model is based on the concept that segregated atoms or ions will alter the potential function at the boundary by virtue of a change in the effective interatomic spacing. Changes in the boundary energy resulting from electronic effects such as charge differences are not considered. This would be expected to be of special significance in ionic materials like alumina where the magnitude and sign of the field associated with the boundary can be strongly influenced by the presence of aliovalent ions [24]. This effect, in addition to the possible creation of point defects in the vicinity of the boundary, would be expected to alter the potential function at the boundary and, in turn, influence the intergranular fracture stress.

Although the finer grain size and pore distribution of the hot-pressed alumina may invalidate any direct comparison with the commercial material, the substantially increased K_{IC} of this alumina is noteworthy. Approximately 50% of the fracture surface exhibited a transgranular (cleavage) crack propagation mode. This suggests that, on the average, the room temperature stresses required to propagate intergranular and transgranular fractures are about equal for the particular microstructural and chemical characteristics represented by this material. Surely, the very clean grain boundaries promote an increased resistance to intergranular fracture. Similarly, the fine grain size should require a larger cleavage fracture stress. In metals, where some dislocation activity is nearly always associated with fracture, the fracture stress is proportional to D^{-n}, where D is the average grain diameter and n is frequently taken to be $\frac{1}{2}$ [18]. Plastic flow is apparently not associated with cleavage fracture in single-crystal alumina (sapphire) except at high temperatures [17], nor has it been reported for cleavage in polycrystalline alumina at ambient temperatures. Wiederhorn has determined that the $(1\,0\,\bar{1}\,0)$ and $(\bar{1}\,0\,1\,2)$ planes in sapphire exhibit the lowest fracture energies [16]. Presumably, a cleavage fracture in a polycrystalline alumina aggregate would tend to propagate preferentially along these planes as well, necessitating reorientation of the crack whenever it intersects a high-angle boundary. The additional energy required for crack reorientation should lead directly to a D^{-n} dependence of fracture stress. However, fractographic observations of cleavage in polycrystalline alumina indicate that a more irrational conchoidal propagation mode can be involved (see Fig. 3). The relationship between the grain size and the energy required to propagate this type of fracture through the structure is unknown, but it may be reasonably assumed that some reorientation across high-angle boundaries will still be required.

Two points should be noted relative to the fracture toughness testing technique employed in this investigation. First, the SENB specimens were notched, not pre-cracked. Pre-cracking was attempted by a microhardness indentation technique [19], but this was unsuccessful. Evans *et al.* [20] has shown that notched specimens tend to give lower K_{IC} values due to the fact that, when the notch is cut, cracks may extend from the base of the notch. This additional flaw length is not considered when determining K_{IC}, resulting in a lower calculated value than actually exists. Secondly, the strain rate employed in the four-point bend testing was quite low. It has been shown in glasses and some ceramics, including alumina, that

slow crack growth can occur during loading [21]. This would produce a larger flaw size under load than was initially present. Then, calculations of K_{IC} based on the initial notch depth would give low values. Therefore, all fracture toughness measurements in this study should be classified as "apparent" K_{IC} values and be viewed as probably constituting a lower limit. In spite of this potential difficulty, the values determined from the as-sintered commercial alumina are in reasonable agreement with the results of other investigations on similar aluminas using SENB specimens [22, 23].

4. Conclusions

In agreement with previous observations, calcium has been shown to segregate readily to the grain boundaries of polycrystalline alumina with enrichment ratios in excess of 10^3, varying with temperature in accordance with equilibrium segregation theory.

The effect of grain-boundary calcium concentrations in the range 0.6 to 1.6 at% on the room temperature fracture behaviour of alumina has been determined for a commercial material containing minimal porosity, no second-phase particles and a uniform grain size of 18 μm. Using SENB specimens in four-point bend loading, average K_{IC} values for predominantly intergranular fracture decreased with increasing calcium segregation from a maximum of 5.08 MN m$^{-3/2}$ at $X_b^{Ca} = 0.006$ to a minimum value of 4.60 MN m$^{-3/2}$ at $X_b^{Ca} = 0.016$. This change is much greater than predicted solely from the effect of such segregation on the inter-atomic spacing at the boundary.

A fine-grained (2 μm) hot-pressed alumina containing very low levels of segregated impurities exhibited substantial amounts of cleavage fracture at room temperature and a high K_{IC} (5.73 MN m$^{-3/2}$). It is suggested that relatively clean grain boundaries resulted in a high boundary fracture stress. Although the influence of grain size on cleavage fracture stress in alumina is unknown, it is presumed that some crack reorientation across a boundary is required and this, in turn, should lead to a D^{-n} dependence of fracture stress. Thus, the fine-grained material with clean boundaries would be expected to exhibit high fracture stresses (and K_{IC}) associated with both intergranular and transgranular fracture modes.

Acknowledgements

The authors gratefully acknowledge Dr R. W. Heckel and Dr B. J. Pletka, whose input to this research through numerous discussions has been most helpful. Dr R. T. Tremper of the General Electric Company was instrumental in providing the aluminas used in this study and A. W. Funkenbusch and L. Bednarz of MTU performed the AES and SAM analyses. This research represents a portion of a programme sponsored by the National Science Foundation under grant DMR76-08467.

References

1. D. McLEAN and L. NORTHCOTT, *J. Iron Steel Inst.* **158** (1948) 169.
2. W. STEVEN and K. BALAJIVA, *ibid.* **193** (1959) 141.
3. P. W. PALMBERG and H. L. MARCUS, *Trans. ASM* **62** (1969) 1016.
4. A. JOSHI and D. F. STEIN, STP499 (ASTM) (1972) 59.
5. *Idem, J. Inst. Metals* **99** (1971) 178.
6. H. L. MARCUS and M. E. FINE, *J. Amer. Ceram. Soc.* **55** (1972) 568.
7. W. C. JOHNSON and D. F. STEIN, *ibid* **58** (1975) 485.
8. A. W. FUNKENBUSCH and D. W. SMITH, *Met. Trans.* **6A** (1975) 2299.
9. M. P. SEAH, *Proc. Roy. Soc. London* A **349** (1976) 535.
10. R. T. TREMPER and R. S. GORDON, *J. Amer. Ceram. Soc.* (1979) (to be published).
11. F. ALBERTS, *Pract. Metallography* **12** (4) (1975) 207.
12. W. F. BROWN Jr and J. E. SRAWLEY, STP 410 (ASTM) (1967) 129.
13. D. McLEAN, "Grain Boundaries in Metals" (Oxford University Press, 1957) p. 118.
14. W. C. JOHNSON, *Met. Trans.* **8A** (1977) 1413.
15. R. S. JUPP and R. W. HECKEL, unpublished research, Michigan Technological University (1978).
16. S. M. WIEDERHORN, *J. Amer. Ceram. Soc.* **52** (1969) 485.
17. S. M. WIEDERHORN, B. J. HOCKEY and D. W. ROBERTS, *Phil. Mag.* **28** (1973) 783.
18. D. McLEAN, "Mechanical Properties of Metals" (Wiley, New York, 1962) p. 255.
19. J. J. PETROVIC, L. A. JACOBSON, P. K. TALTY and A. K. VASUDEVAN, *J. Amer. Ceram. Soc.* **58** (1975) 113.
20. A. G. EVANS, M. LINZER and L. R. RUSSELL, *Mat. Sci. Eng.* **15** (1974) 253.
21. S. M. WIEDERHORN, *Fract. Mech. Ceram.* **2** (1974) 613.
22. L. A. SIMPSON, *J. Amer. Ceram. Soc.* **56** (1973) 7.
23. H. HÜBNER and W. JILLEK, *J. Mater. Sci.* **12** (1977) 117.
24. K. L. KLIEWER and J. S. KOEHLER, *Phys. Rev.* **140** (1965) 1226.

Received 15 March and accepted 10 May 1979.